From Valence Trapped to Valence Delocalized by Bridge State Modification in Bis(triarylamine) Radical Cations: Evaluation of Coupling Matrix Elements in a Three-Level System

Christoph Lambert,* Stephan Amthor, and Jürgen Schelter

Institut für Organische Chemie, Bayerische Julius-Maximilans-Universität Würzburg, Am Hubland, D-97074 Würzburg, Germany

Received: April 8, 2004

This paper presents an analysis of the visible/near-infrared (vis/NIR) spectra of four bis(triarylamine) radical cation mixed valence systems with varying bridge units in the framework of the generalized Mulliken−Hush theory. We outline how to apply a three-level model by using both computational AM1-CI derived as well as experimental transition moments and energies in order to extract electronic coupling matrix elements. The most important outcome is that the much simpler two-level model is a good approximation only if the adiabatic dipole moment difference between the terminal states is large compared to the transition moments associated with the bridge state. This implies that the two-level model is only applicable to mixed valence compounds in the Robin−Day class II with strongly localized redox states if qualitative correct values are desired. We demonstrate that both the spectral features and the potential energy surface of the mixed valence compounds can solely be tuned by bridge state modification reaching from asymmetrically localized to symmetrically localized and from a single minimum potential to a triple minimum potential. For the particular case of an anthracene bridge, we show that solvent induced symmetry breaking has a dramatic influence on the spectral characteristics.

Introduction

In this paper, we will analyze the visible/near-infrared (vis/NIR) spectra of four bis(triarylamine) radical cation mixed valence (MV) systems with varying bridge units in the framework of the generalized Mulliken−Hush (GMH) theory.[1−3] We will outline how to apply a three-level model by using both computational AM1-CI derived as well as experimental transition moments and energies in order to extract electronic coupling matrix elements which serve as a measure of the electronic communication between different states. Finally, we will show that valence delocalization can solely be induced by bridge state modification, a topic which has attracted much interest recently in terms of the Robin−Day class II−III transition.[4−12]

Although simple in its concept and application, the Marcus−Hush theory is a very powerful method for analyzing the charge transfer (CT) spectra of both inorganic and organic mixed valence compounds.[13−18] The MV compounds are comprised of two redox centers of different oxidation states that are connected by a bridge. These MV species are used as basic systems in which electron transfer can be studied by analyzing the associated CT bands. In the simplest case, this analysis starts off with the construction of two adiabatic potential energy surfaces (PESs) from the diagonalization of two diabatic (formally noninteracting) potentials in a 2×2 secular determinant (eq 1), where V is the electronic coupling between the diabatic states. If one assumes these diabatic potentials to be degenerate and to have a quadratic dependence on an asymmetric electron transfer (ET) coordinate, the potentials are those in Figure 1. Optical excitation (usually in the NIR region) from one minimum of the ground state PES causes the transfer of an electron or a hole from one redox center to the other. The absorption associated with this excitation is called an intervalence charge transfer (IV-CT). Provided that quadratic potentials with the force constant λ (i.e., the Marcus reorganization energy) are used, the IV-CT energy equals λ. Analysis of this absorption using eq 2 yields the electronic coupling $V_{\text{two-level}}$. In this equation, μ_{ga} is the transition moment of the IV-CT and $\Delta\mu_{12}$ is the diabatic transition moment difference between both diabatic minima of the PES (see Figure 1). While μ_{ga} is readily accessible by integration of the IV-CT band (eq 3), $\Delta\mu_{12}$ cannot be determined directly. However, according to the GMH theory, the diabatic dipole moment difference can be traced back to purely adiabatic (measurable) quantities by eq 4,[1−3] where $\Delta\mu_{ag}$ is the adiabatic dipole moment difference which, in some cases, can be determined by Stark spectroscopy[19−21] or quantum

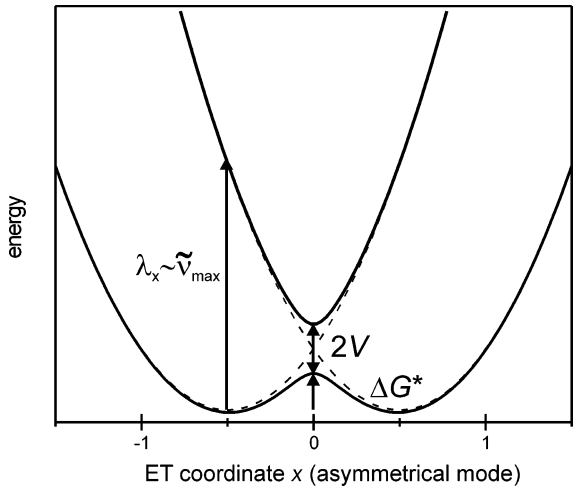

Figure 1. Adiabatic (solid lines) and diabatic (dashed lines) potential energy surfaces for a degenerate two-level system.

* Corresponding author. E-mail: lambert@chemie.uni-wuerzburg.de.

10.1021/jp048449s CCC: $27.50
Published on Web 07/14/2004

chemical methods.[22] In most cases, however, this adiabatic quantity or the diabatic dipole moment difference is estimated by e × *r*, where *r* is the geometrical distance of redox centers. However, quite recently, Nelsen et al. emphasized that using the nitrogen−nitrogen distance is quite a poor approach for estimating either $\Delta\mu_{12}$ or $\Delta\mu_{ag}$ in bis(triarylamine) systems.[23] For derivatives with very strong electronic coupling ($\lambda \sim 2V$) and asymmetric IV-CT bands, a two-level, two-mode analysis (one asymmetric and one symmetric ET mode) was used by Coropceanu et al.[24,25] within a dynamic vibronic model and by us[26] within a semiclassical model which allows the determination of *V* without any assumption about $\Delta\mu_{12}$ or $\Delta\mu_{ag}$. However, in the usual cases of weak coupling ($\lambda \gg 2V$), IV-CT bands are symmetrically Gaussian shaped and the exact value of either $\Delta\mu_{12}$ or $\Delta\mu_{ag}$ is necessary for a proper analysis.

$$\begin{vmatrix} H_{11} - \epsilon & V_{\text{two-level}} \\ V_{\text{two-level}} & H_{22} - \epsilon \end{vmatrix} = 0 \tag{1}$$

with $H_{11} = \lambda x^2$ and $H_{22} = \lambda(1 - x)^2$

$$V_{\text{two-level}} = \frac{\mu_{ga}\tilde{\nu}_{\max}}{\Delta\mu_{12}} \tag{2}$$

$$\mu_{ga} = 0.095\,84\sqrt{\frac{\int \epsilon(\tilde{\nu})\,d\tilde{\nu}}{\tilde{\nu}_{\max}}} \tag{3}$$

$$\Delta\mu_{12} = \sqrt{\Delta\mu_{ag}{}^2 + 4\mu_{ga}{}^2} \tag{4}$$

Innumerable systems have been analyzed by applying the two-level approach in order to extract the electronic coupling and to correlate this coupling with, for example, the type of redox centers, the bridge type or length,[6,15,18] the influence of the temperature[25,27] or the solvent,[28−31] and gegenions.[32,33] In many recent studies, the electron transfer between terminal redox centers mediated by bridge units was investigated.[34−44] In most of these studies, it was assumed that the direct electronic coupling between the terminal states is negligible (tight binding approximation). However, in some MV compounds, it appears that besides a strong IV-CT band a second optical transition is visible.[43,45−47] If this second band also has some charge transfer character, it seems appropriate to include this band in an extended analysis using a three-level approach (see Figure 2) in which both direct and bridge mediated coupling are significant. In a recent study, we presented radical cation systems based on two triarylamine redox centers that are connected by a conjugate *p*-dialkynylarene bridge (compounds **1**$^+$−**3**$^+$, see Chart 1) in which besides an IV-CT band ($\tilde{\nu}_a$ in Figure 2) a second band is visible ($\tilde{\nu}_b$ in Figure 2).[47]

We have interpreted this second band to be associated with a triarylamine to bridge hole transfer, and we have applied a three-level model to analyze the spectra. In Figure 2, one has to take into account that the traditional Marcus−Hush ET coordinate is associated with an averaged asymmetric vibrational mode (*x*), while the mode that localizes the hole at the bridge is an averaged symmetrical mode (*y*). The potentials associated with this symmetrical mode are given as dashed lines in Figure 2. By this way, we could show that depending on the energetic level and reorganization energy of the bridge two alternative ET pathways are conceivable: one in which superexchange (coherent ET) directly occurs between the two triarylamine redox centers and another pathway in which the bridge serves as an intermediate state (incoherent hopping mechanism) (see Scheme 1). In the present study, we will present the additional system **4**$^+$ where the triarylamine redox centers have been modified together with studies concerning the solvent influences of the radical cation spectra. Comparison with the recent data and with semiempirical AM1 computations prompted us to reanalyze the older data set which led to different results in the particular case with anthracene bridges. We will show that, in contrast to our earlier interpretation, the ground state of the radical cations **3**$^+$ and **4**$^+$ is bridge centered in CH_2Cl_2 solution, as indicated in Figure 3. In this context, it seems necessary to analyze the three-level model and the parameters that enter this model in more detail.

Results and Discussion

A. Evaluation of Electronic Couplings (*V*'s) by the GMH Theory. The GMH theory is based on a unitary transformation of matrices containing adiabatic (measurable) quantities into matrices containing diabatic quantities and vice versa.[1,2] The GMH theory has been successfully used in the past for analyzing IV-CT spectra from either experimental or computational data.[22,48−50] In most cases, the analysis was based on two-level systems, but also some investigations of three-level systems are known. The first step of the GMH theory is to find the matrix **C** that diagonalizes the adiabatic matrix ($\boldsymbol{\mu}_{\text{adiab}}$) according to $\boldsymbol{\mu}_{\text{diab}} = \mathbf{C}^t\boldsymbol{\mu}_{\text{adiab}}\mathbf{C}$ with

$$\boldsymbol{\mu}_{\text{adiab}} = \begin{pmatrix} 0 & \mu_{ga} & \mu_{gb} \\ \mu_{ga} & \mu_{aa} - \mu_{gg} & \mu_{ab} \\ \mu_{gb} & \mu_{ab} & \mu_{bb} - \mu_{gg} \end{pmatrix}$$

and

$$\boldsymbol{\mu}_{\text{diab}} = \begin{pmatrix} 0 & 0 & 0 \\ 0 & \mu_{22} - \mu_{11} & 0 \\ 0 & 0 & \mu_{33} - \mu_{11} \end{pmatrix}$$

The matrix $\boldsymbol{\mu}_{\text{adiab}}$ contains the adiabatic transition moments for two different excited states a and b which are the IV-CT (μ_{ga}) and bridge states (μ_{gb}) in the radical cations **1**$^+$ and **2**$^+$ mentioned above as well as the transition moment between these excited states (μ_{ab}). The matrix $\boldsymbol{\mu}_{\text{adiab}}$ also contains the differences of the adiabatic dipole moments of the ground state minimum and either the first excited state ($\mu_{aa} - \mu_{gg}$) (IV-CT state in **1**$^+$ and **2**$^+$) or the second excited state ($\mu_{bb} - \mu_{gg}$) (bridge state in **1**$^+$ and **2**$^+$). The diagonalization then yields the diabatic dipole moment differences of the ground state minimum and either the first (IV-CT in **1**$^+$ and **2**$^+$) state ($\mu_{22} - \mu_{11}$) or the second (bridge in **1**$^+$ and **2**$^+$) state ($\mu_{33} - \mu_{11}$). The second step of the GMH theory is to apply the same unitary transformation to the adiabatic energy matrix $\mathbf{H}_{\text{diab}} = \mathbf{C}^t\mathbf{H}_{\text{adiab}}\mathbf{C}$ with

$$\mathbf{H}_{\text{adiab}} = \begin{pmatrix} 0 & 0 & 0 \\ 0 & \tilde{\nu}_a & 0 \\ 0 & 0 & \tilde{\nu}_b \end{pmatrix}$$

and

$$\mathbf{H}_{\text{diab}} = \begin{pmatrix} H_{11} & V_{12} & V_{13} \\ V_{12} & H_{22} & V_{23} \\ V_{13} & V_{23} & H_{33} \end{pmatrix}$$

The matrix contains the adiabatic transition energies of the first excited state ($\tilde{\nu}_a$) (IV-CT state in **1**$^+$ and **2**$^+$) and the second excited state ($\tilde{\nu}_b$) (bridge state in **1**$^+$ and **2**$^+$) and yields after transformation the diabatic energy matrix from which the

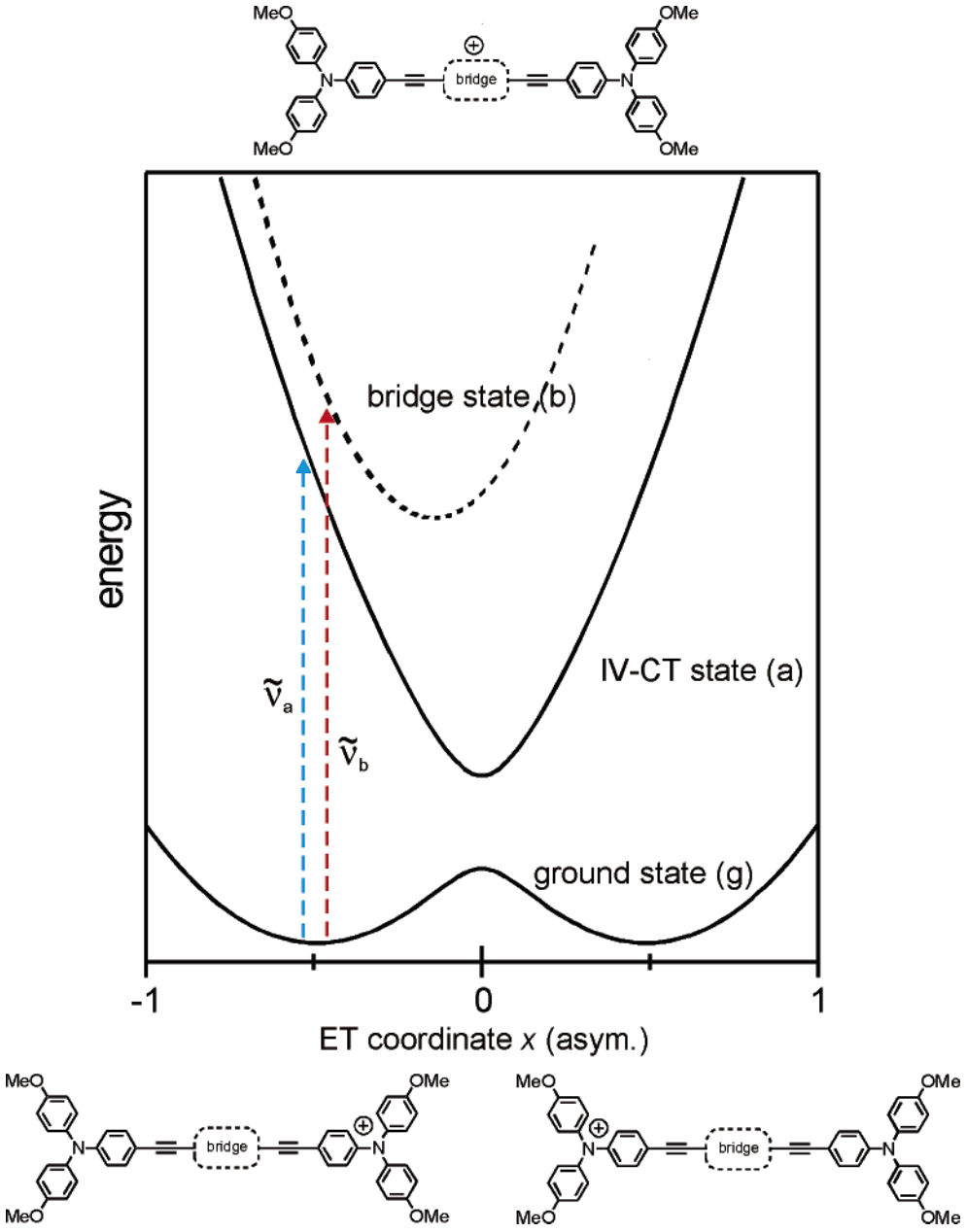

Figure 2. Adiabatic potential energy surfaces for a three-level system with the bridge state being higher in energy than the IV-CT state. The solid lines refer to the asymmetric *x* coordinate, while the dashed curve refers to the symmetric *y* coordinate which is perpendicular to the *x* coordinate. It is important to note that the minimum of the bridge state potential is shifted vs the ground state potentials along the *y* axis.

electronic couplings V_{12}, V_{13}, and V_{23} can directly be obtained. In this way, the electronic couplings solely depend on the transition moments and the band energies and, thus, on the initial deconvolution of experimental spectra by, for example, Gaussian functions.

While the adiabatic transition energies and transition moments are readily available from band integration (see above), problems arise in the determination of the adiabatic dipole moment differences. In principle, Stark spectroscopy can be applied to measure the dipole moments of excited states.[19] However, this proved to be difficult because MV radical ions have to be immobilized in glass matrices. Although much less reliable, the most common way is to estimate either the diabatic or the adiabatic electron transfer distance by the redox center separation (r) as we have done in our recent contributions. Nelsen et al. quite recently pointed out that this edge-to-edge approximation is rather poor and yields much too long effective distances and, thus, too large dipole moment differences, $\mu_{aa} - \mu_{gg} = e \times r$.[23] An alternative way is to estimate the dipole moments by quantum chemical calculations.[22] However, while density functional theory (DFT) computations systematically overemphasize charge delocalization[51] and, therefore, yield too small dipole moments,[24,25] unrestricted Hartree−Fock (UHF) calculations (both ab initio and AM1) overestimate charge localization together with high spin contamination and exaggerate the dipole moments.[6,52] Therefore, for a quantitative evaluation of the electronic coupling of $\mathbf{1}^+-\mathbf{3}^+$, we used the AM1-CI method to estimate the dipole moments of the ground and excited states. This method is based on the Dewar's restricted Hartree−Fock (RHF) half-electron method[53] and does not suffer from spin contamination. Although we have no proof that this method yields quantitative, accurate results, its outcome is physically more convincing than either UHF or DFT computations. However, before we present and discuss these results, we will try to give a general analysis of the electronic coupling elements

CHART 1

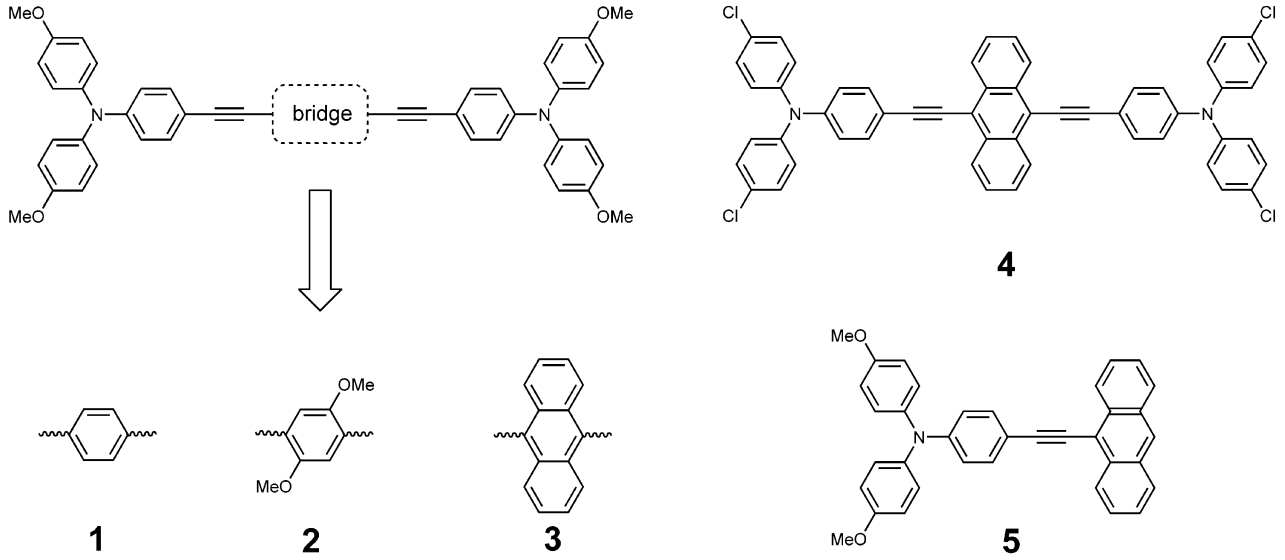

SCHEME 1

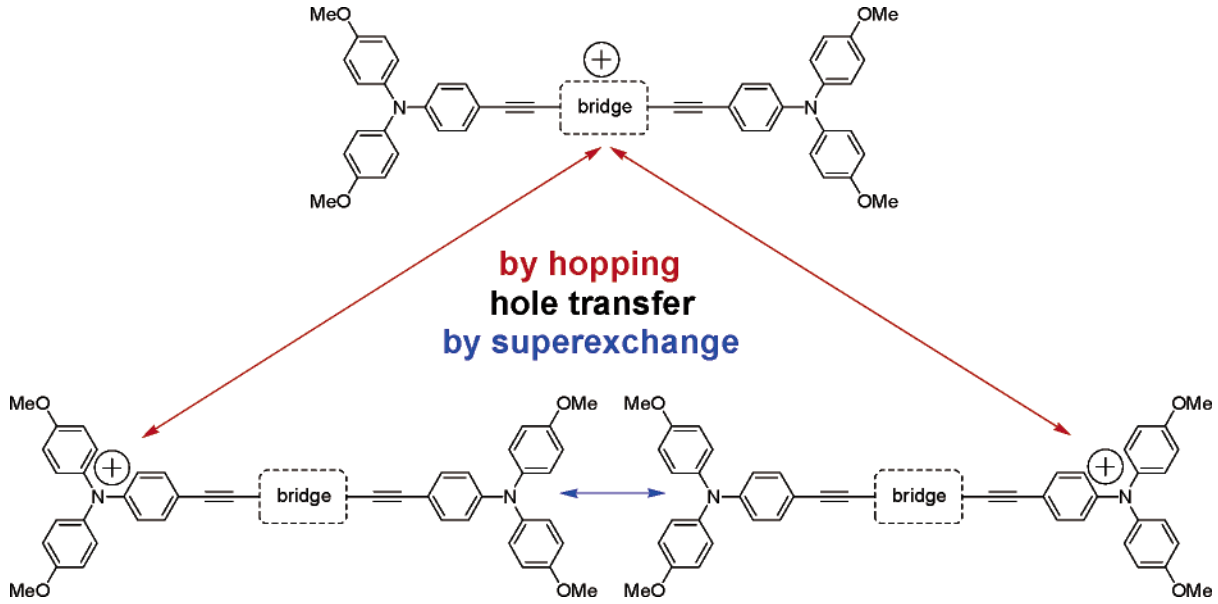

depending on the transition moments and the relative energies of the IV-CT and bridge states within the three-level model.

In the following, we refer to a state diagram like that given in Figure 2; that is, the bridge state is energetically situated above the IV-CT state. In Figure 4a−c, the relative electronic couplings (see matrix $\mathbf{H}_{diab}$) derived from the GMH analysis are given depending on the ratio μ_{ab}/μ_{gb} (see matrix $\boldsymbol{\mu}_{diab}$). The sum of $|\mu_{ab}| + |\mu_{gb}|$ was kept constant for three different values of $\Delta\mu_{ag} = \mu_{aa} - \mu_{gg}$. Because $\Delta\mu_{ag}$ is the larger the more localized the charge of the MV compound is, and because $\Delta\mu_{ag} = 0$ for a completely delocalized MV species, the three plots for $\Delta\mu_{ag} = 75$, $\Delta\mu_{ag} = 25$, and $\Delta\mu_{ag} = 10$ reflect a different degree of charge localization. The sum of $|\mu_{ab}| + |\mu_{gb}|$ was chosen to be twice that of μ_{ga}, a ratio supported by AM1-CI computations, as outlined in the next section. The dipole moment difference $\mu_{bb} - \mu_{gg}$ was set to $\Delta\mu_{ag}/2$ because the bridge state (b) has a symmetrical charge distribution in its vibrationally relaxed state with $\mu_{bb} = 0$. In the next section, we will show that this approximation is reasonably well fulfilled. Furthermore, we fixed the relative transition energies at $\tilde{\nu}_a = 1$ and $\tilde{\nu}_b = 2$. These relative values seem to be reasonable, as all systems which are known to us show a bridge band that is considerably higher in energy than the IV-CT band.

For a three-level model, two different physical situations arise depending on whether the number of positive adiabatic transition moments is even or odd. The resulting number of positive electronic couplings (V's) then is odd or even, respectively, if $\mu_{gg} < 0$ and $\mu_{aa} > 0$. As the sign of both the transition moments and the electronic couplings refers to a phase relation, only the number of positive or negative elements is meaningful and not its assignment to specific matrix elements.[1] These two distinguishable cases are depicted in Figure 4a−c on both sides of the diagrams for a positive (right-hand side) and negative (left-hand side) μ_{ab}/μ_{gb} ratio. For the couplings, only the absolute magnitude is given. From these plots, it is obvious that for large values of $\Delta\mu_{ag}$ (Figure 4a) the two-level coupling ($V_{two-level}$) (see eq 2) is a reasonably good approximation for V_{12}. It is important to note that in this case the agreement is only weakly dependent on the ratio μ_{ab}/μ_{gb}. However, for $\Delta\mu_{ag}/(|\mu_{ab}| + |\mu_{gb}|)$ ratios being much smaller than ~5, the deviation becomes strong (Figure 4b,c) and the three-level model has to be applied for an accurate description.

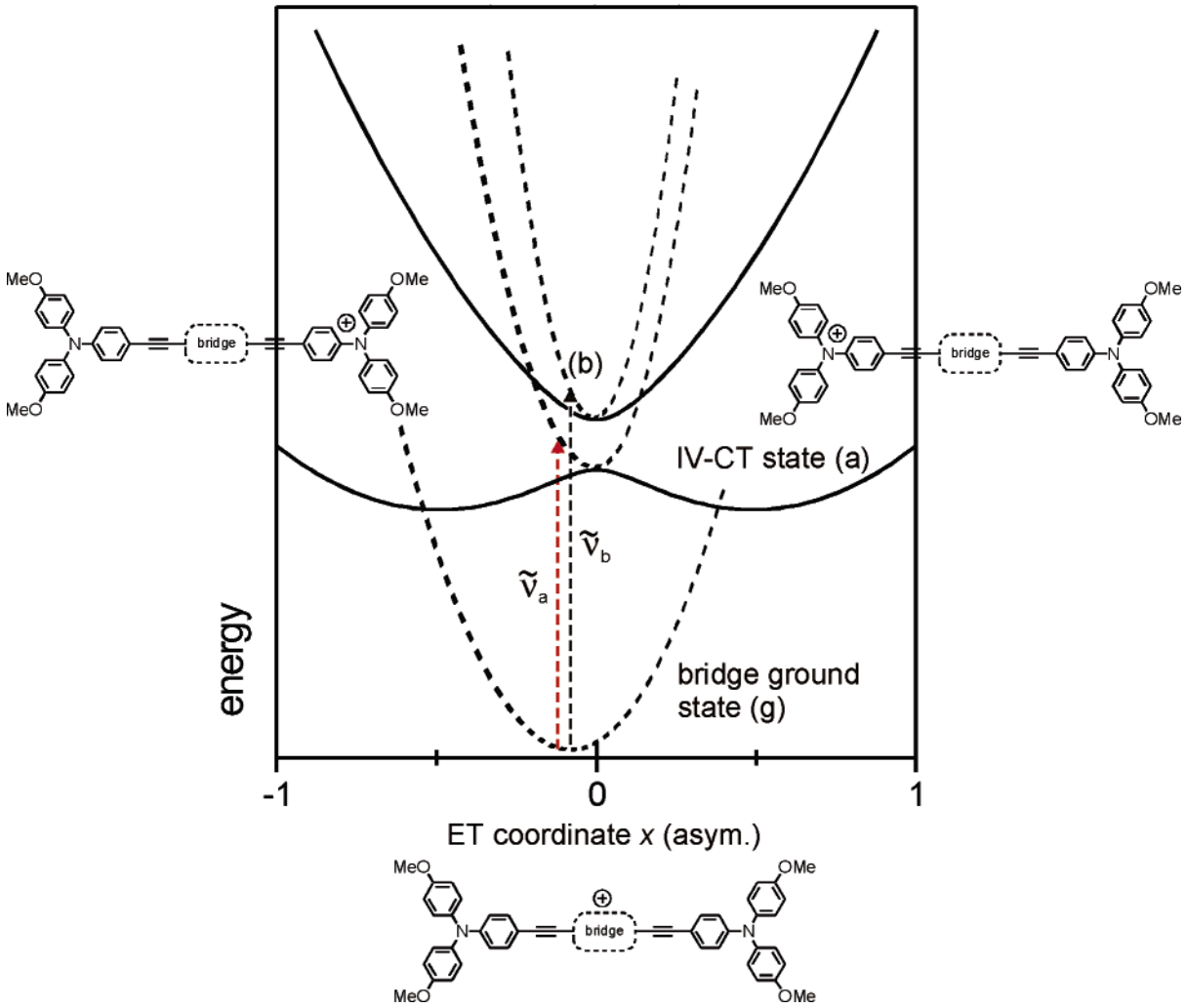

Figure 3. Adiabatic potential energy surfaces for a three-level system with the bridge state being the ground state. The solid lines refer to the asymmetric *x* coordinate, while the dashed curve refers to the symmetric *y* coordinate which is perpendicular to the *x* coordinate. It is important to note that the minimum of the ground state potential is shifted vs the excited state potentials along the *y* axis.

To gain more insight into the dependence of V on the transition energies, we plotted V in Figure 4d for a given set of parameters depending on the ratio $\tilde{\nu}_b/\tilde{\nu}_a$. The first observation is that all electronic couplings depend linearly on the energy ratio, with V_{12} being less dependent than V_{13} and V_{23}, and the second observation is that the deviation of $V_{\text{two-level}}$ from V_{12} increases with an increasing $\tilde{\nu}_b/\tilde{\nu}_a$ ratio, much in contrast to our initial suggestion. For $\Delta\mu_{ag}$ values smaller than 75, the deviations are even stronger. We stress that the above-mentioned analysis does not apply to real systems because in practice one cannot vary one parameter while keeping all the others constant. The analysis merely serves to illustrate the quite different behaviors of the two-level and three-level models.

B. AM1-CISD Computations. As we have mentioned above, Dewar's half-electron method does not suffer from spin contamination as UHF wave functions do in the cases of triarylamine radical cations. Therefore, we used an AM1-CI expansion with singles and doubles excitations (CISD) with an active orbital window comprising four doubly occupied, one singly occupied, and three empty orbitals for the optimization of the radical cation ground states of $\mathbf{1}^+$, $\mathbf{2}^+$, and $\mathbf{3}^+$. For computing the transition energies and transition moments that are necessary for a proper three-level analysis using the GMH theory, we used the gas phase optimized structures and calculated single points at the AM1-CISD level including the conductor-like screening model (COSMO) method for simulating an environment of a solvent with $\epsilon = 2.0$.[54] The computed results are given in Table 1 in the form of the respective matrices. At this point, we stress that all computed values may only show trends and cannot safely be taken as accurate even though the solvent was taken into account when computing the excited state properties at the geometry of the gas phase optimized structures.

For $\mathbf{1}^+$, the AM1-CISD optimization gives an asymmetric radical cation ground state structure with the hole localized primarily at the triarylamine moiety. This can be seen from the large ground state dipole moment (39.3 D)[55] which refers to a displacement of charge from the bridge center by ~8.2 Å. The asymmetry is obvious when looking at the bond lengths in Chart 2. The part where the hole is localized shows a somewhat stronger quinoid structure, while the neutral part is more benzenoid. The Coulson charge differences between the radical cation and its neutral counterpart also show positive charge concentration at the left triarylamine moiety.

Much in contrast, $\mathbf{3}^+$ turned out to be symmetrical (C_{2h} symmetry) with the charge being mainly localized at the anthracene bridge and at the attached alkyne groups, as can be seen from its vanishing ground state dipole moment, the Coulson charge differences (Chart 2), and the symmetrical bond lengths arrangement. Below, we will give experimental evidence that $\mathbf{3}^+$ is indeed a symmetrical valence delocalized radical cation. The charge distribution of the radical cation $\mathbf{2}^+$ is intermediate

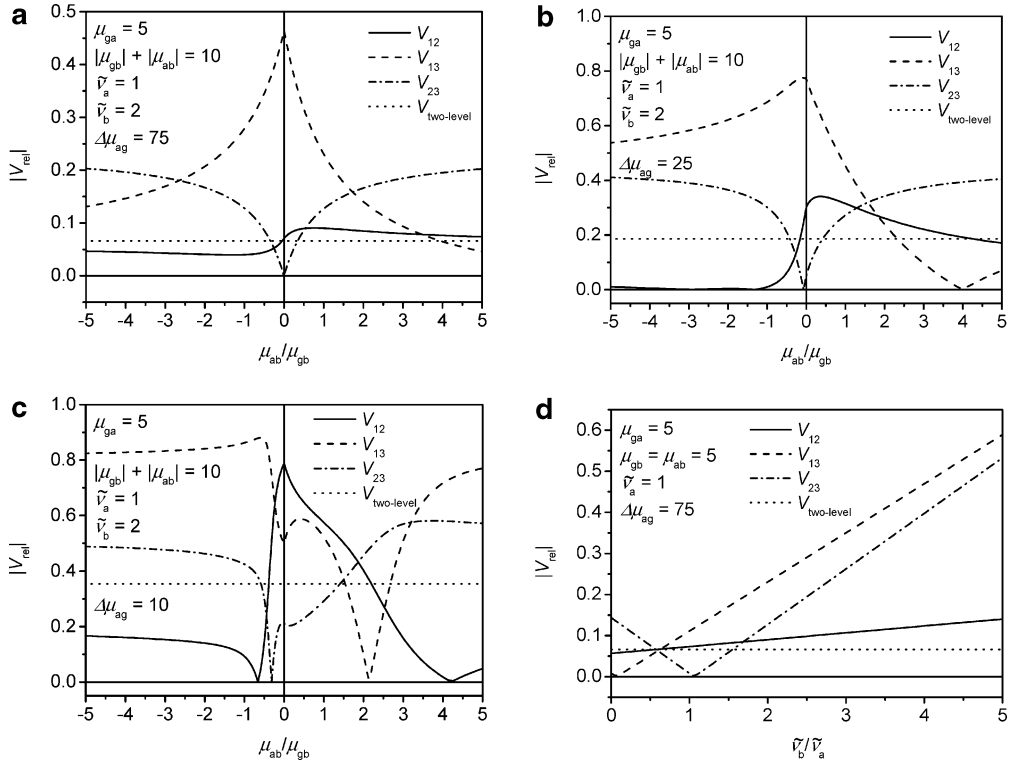

Figure 4. (a−c) Absolute value of electronic coupling as a function of the ratio μ_{ab}/μ_{gb} for three different $\Delta\mu_{ag}$ values. (d) Absolute value of electronic coupling as a function of the ratio $\tilde{\nu}_b/\tilde{\nu}_a$.

with $\mu_{gg} = -21.3$ D, which refers to a displacement of only 4.3 Å. This effect is clearly due to the methoxy donor substituents which favor positive charge delocalization into the bridge and, thus, reduce the dipole moment.[56]

The adiabatic dipole moments (μ_{aa} and μ_{bb}) of the two lowest excited states of $\mathbf{1}^+$ and of $\mathbf{2}^+$ easily identify them as IV-CT and bridge states, respectively. The adiabatic dipole moment differences ($\Delta\mu_{ag} = \mu_{aa} - \mu_{gg}$) in a solvent with $\epsilon = 2.0$ decrease from $\mathbf{1}^+$ (63.4 D) over $\mathbf{2}^+$ (32.3 D) to $\mathbf{3}^+$ (0.0 D) which also reflects the increasing delocalization of positive charge into the bridge with increasing donor character of the bridge. The dipole moment difference $\mu_{bb} - \mu_{gg}$ is in fact somewhat larger for $\mathbf{1}^+$ ($\mu_{bb} - \mu_{gg} = 43.3$ D, $\Delta\mu_{ag}/2 = 31.7$ D) and for $\mathbf{2}^+$ ($\mu_{bb} - \mu_{gg} = 17.5$ D, $\Delta\mu_{ag}/2 = 16.2$ D) than its approximation, $\Delta\mu_{ag}/2$, which was used for the analyses in Figure 4 in a solvent with $\epsilon = 2.0$. Nevertheless, this approximation seems to be reasonably good.

The AM1 computed energies of the IV-CT transition and the bridge transition are in very good agreement with experiment for $\mathbf{1}^+$ and $\mathbf{2}^+$ but differ strongly for the transition observed in $\mathbf{3}^+$. This transition in $\mathbf{3}^+$ might be termed a "bridge to triarylamine" CT. The bad agreement of the AM1 calculated transition energy and the experimental value might be due to an underestimation of the triarylamine radical cation stability versus the anthracene radical cation stability by the AM1 method.[57] Much in contrast, the computed transition moments of the IV-CT bands of $\mathbf{1}^+$ and $\mathbf{2}^+$ are much higher than the experimental values. However, transition moments are a quantity that are generally difficult to calculate accurately even at a much higher level of theory. When going from $\mathbf{1}^+$ over $\mathbf{2}^+$ to $\mathbf{3}^+$, one generally observes a monotonic trend of all transition moments. The fact that μ_{ga} and μ_{ab} are different reflects that the Condon approximation (μ being independent of the nuclear coordinates) is not valid in these cases.

For $\mathbf{3}^+$, the μ_{ga} transition ($B_g \rightarrow B_u$) is in good agreement with the experiment but μ_{gb} vanishes because this transition is forbidden for symmetry reasons ($B_g \rightarrow B_g$) within C_{2h} symmetry. In contrast, the excitation from the first excited state to the second excited state is strongly allowed ($B_u \rightarrow B_g$). This excitation can be viewed as an excited state IV-CT transition near the geometry of the excited transition state for the thermal degenerate triarylamine hole transfer. From Figure 3, one can see that owing to the shift of the ground state PES along the symmetric coordinate the g → a excitation meets the excited PES at a point higher than the transition state.

The diabatic quantities obtained by the GMH unitary transformation of the adiabatic quantities are also collected in Table 1. While for $\mathbf{1}^+$ the diabatic dipole moment differences are $\mu_{22} - \mu_{33} = 40.6$ D and $\mu_{33} - \mu_{11} = 42.5$ D, these dipole differences are much different for $\mathbf{2}^+$ (42.6 and 22.0 D). The dipole moment difference is $\mu_{22} - \mu_{11} = 83.1$ D for $\mathbf{1}^+$ and 64.6 D for $\mathbf{2}^+$. The quantity for $\mathbf{3}^+$ to compare with is $\mu_{33} - \mu_{22} = 70.6$ D. The corresponding adiabatic quantities are much smaller, $\Delta\mu_{ag} = \mu_{aa} - \mu_{gg} = 63.4$ D ($\mathbf{1}^+$) and 32.3 D ($\mathbf{2}^+$). The dipole moment difference estimated from the N−N distance (19.2 Å in, e.g., $\mathbf{1}^+$) is much larger: 92.1 D. It is obvious that taking this dipole moment difference as either the adiabatic ($\mu_{aa} - \mu_{gg}$) or the diabatic ($\mu_{22} - \mu_{11}$) dipole moment difference involves a major error which is stronger the more delocalized the charge is into the bridge.

According to Matyushov and Voth[58] as well as to Coropceanu et al.,[24] half of the diabatic transition dipole moment difference ($\mu_{22} - \mu_{11}$) is equal to the adiabatic transition moment (μ_{ga}) at the transition state of the thermal ET within the two-level model. In fact, for $\mathbf{1}^+$-**TS**, $(\mu_{22} - \mu_{11})/2 = 32.5$ D is somewhat larger than $\mu_{ga} = 25.4$ D. However, this approximation cannot be used to estimate the $(\mu_{22} - \mu_{11})/2$ value of the relaxed asymmetric structure of $\mathbf{1}^+$ which is distinctly higher (41.6 D).[59] For $\mathbf{3}^+$, this relation is also approximately fulfilled for the excited state PES: $(\mu_{33} - \mu_{22})/2 = 35.3$ D $\sim \mu_{ab} = 33.1$ D.

From Figure 4a−c, it is evident that the two-level model is generally a good approximation only if the adiabatic dipole

TABLE 1: Adiabatic and Diabatic Energy (cm^{-1}) and Dipole Moment (D) Matrices for 1^+, 2^+, and 3^+ Computed at the AM1-CISD Level[a]

		1^+	
$\mathbf{H}_{adiab}$	0.0	$\tilde{\nu}_a = 4140$ (6940) [8060]	$\tilde{\nu}_b = 10\,260$ (12 950) [12 000]
$\boldsymbol{\mu}_{adiab}$[b]	$\mu_{gg} = -31.5$ (−39.3)	$\mu_{ga} = 26.3$ (20.8) [6.2]	$\mu_{gb} = 5.7$ (6.5) [4.7]
		$\mu_{aa} = 26.6$ (24.1)	$\mu_{ab} = 19.6$ (14.2)
			$\mu_{bb} = -4.6$ (+4.0)
$\boldsymbol{\mu}_{diab}$	$\mu_{11} = -10.2$ (−6.3){−0.9}	$\mu_{22} = 76.6$ (76.8) {71.6}	$\mu_{33} = 18.7$ (36.2) {36.0}
$\mathbf{H}_{diab}$[c]		$V_{12} = 1120$ (1920) {1000}	$V_{13} = 1030$ (250) {560}
$V_{two-level} = 1390$ (1900) {770}			$V_{23} = 2400$ (2430) {1570}
		2^+	
$\mathbf{H}_{adiab}$	0.0	$\tilde{\nu}_a = 5360$ (5880) [6520]	$\tilde{\nu}_b = 10\,560$ (11 020) [10 610]
$\boldsymbol{\mu}_{adiab}$[b]	$\mu_{gg} = -13.3$ (−21.3)	$\mu_{ga} = 23.7$ (22.4) [9.7]	$\mu_{gb} = 2.6$ (3.9) [6.8]
		$\mu_{aa} = 9.0$ (11.0)	$\mu_{ab} = 20.6$ (17.3)
			$\mu_{bb} = -4.4$ (−3.8)
$\boldsymbol{\mu}_{diab}$	$\mu_{11} = -18.7$ (−12.3) {−3.0}	$\mu_{22} = 46.9$ (52.3) {46.7}	$\mu_{33} = 3.0$ (9.7) {6.1}
$\mathbf{H}_{diab}$[c]		$V_{12} = 700$ (1500) {1910}	$V_{13} = 3750$ (2620) {770}
$V_{two-level} = 2430$ (2390) {1680}			$V_{23} = 3190$ (2820) {1760}
		3^+	
$\mathbf{H}_{adiab}$	0.0	$\tilde{\nu}_a = 10040$ (9550) [4640]	$\tilde{\nu}_b = 13\,060$ (12 470) [6500][f]
$\boldsymbol{\mu}_{adiab}$[d,e]	$\mu_{gg} = 0.0$ (0.0)	$\mu_{ga} = 12.1$ (12.2) [14.1]	$\mu_{gb} = 0.0$ (0.0)
		$\mu_{aa} = 0.0$ (0.0)	$\mu_{ab} = 34.9$ (33.1)
			$\mu_{bb} = 0.0$ (0.0)
$\boldsymbol{\mu}_{diab}$	$\mu_{11} = 0.0$ (0.0)	$\mu_{22} = -36.9$ (−35.3) {−36.0}	$\mu_{33} = 36.9$ (35.3) {36.0}
$\mathbf{H}_{diab}$[e]		$V_{12} = 2860$ (2860) {1660}	$V_{13} = 2860$ (2860) {1660}
			$V_{23} = 810$ (710) {430}
		1^+-TS	
$\mathbf{H}_{adiab}$	0.0	$\tilde{\nu}_a = 3930$ (3990)	$\tilde{\nu}_b = 11\,690$ (11 600)
$\boldsymbol{\mu}_{adiab}$[d,e]	$\mu_{gg} = 0.0$ (0.0)	$\mu_{ga} = 26.0$ (25.4)	$\mu_{gb} = 0.0$ (0.0)
		$\mu_{aa} = 0.0$ (0.0)	$\mu_{ab} = 20.2$ (20.3)
			$\mu_{bb} = 0.0$ (0.0)
$\boldsymbol{\mu}_{diab}$	$\mu_{11} = -32.9$ (−32.5)	$\mu_{22} = 32.9$ (32.5)	$\mu_{33} = 0.0$ (0.0)
$\mathbf{H}_{diab}$[e]		$V_{12} = 240$ (270)	$V_{13} = 4010$ (4000)
			$V_{23} = 4010$ (4000)

[a] **1^+-TS** refers to the gas phase structure of the symmetrical ET transition state. Values in parentheses are calculated for a solvent with $\epsilon = 2.0$. Values in square brackets are experimental values in CH_2Cl_2. Diabatic values in braces are derived from the experimental adiabatic values and, where lacking, from the corresponding computed adiabatic values in the solvent. [b] Odd number of positive off-diagonal transition moments. [c] Even number of positive coupling elements. [d] The diagonal elements were computed to be close to zero but set to 0.0 for symmetry reasons for the subsequent GMH analysis. [e] The sign of the off-diagonal elements does not lead to physically distinguishable situations. [f] Estimated.

moment difference ($\Delta\mu_{ag}$) is large compared to the other transition moments. That is why for $\mathbf{1}^+$ there is good agreement between the computed $|V_{12}|$ and $V_{two-level}$ values, while there is a considerably worse agreement for $\mathbf{2}^+$ in which $\Delta\mu_{ag}$ is much smaller. If we use the experimental energies and transition moments where available (see next section) and the computed transition moments (μ_{ab}'s) and dipole moments (μ_{gg}, μ_{aa}, and μ_{bb}) for the missing values, we obtain $|V_{12}|$ couplings that are in reasonably good agreement with the $V_{two-level}$ values for both $\mathbf{1}^+$ and $\mathbf{2}^+$ because the experimental μ_{ga} value is much smaller than the computed values and now considerably smaller than $\Delta\mu_{ag}$. The GMH analysis also revealed that for $\mathbf{1}^+$ and $\mathbf{2}^+$ V_{12} (which refers to the coupling between the triarylamine centered states) is intermediate between V_{13} and V_{23}.[60]

The V_{12} coupling is much stronger for $\mathbf{2}^+$ than for $\mathbf{1}^+$ which is primarily due to the smaller adiabatic dipole moment difference ($\Delta\mu_{ag}$). The strong differences between $\mathbf{1}^+$ and $\mathbf{2}^+$ are not apparent from the energies or transition moments directly but are visible if one considers the adiabatic dipole moments (μ_{gg}, μ_{aa}, and μ_{bb}). The different behavior of $\mathbf{1}^+$ and $\mathbf{2}^+$ reflects the stronger charge delocalization into the donor substituted bridge in $\mathbf{2}^+$ compared to $\mathbf{1}^+$. If the donor character of the bridge is even stronger, as in $\mathbf{3}^+$, the bridge state becomes the ground state minimum (Figure 3) and the system can be viewed as valence delocalized.

C. Experimental vis/NIR Spectra of 1^+, 2^+, 3^+, and 4^+. The vis/NIR spectra of $\mathbf{1}^+$ and $\mathbf{2}^+$ in CH_2Cl_2 have already been described in ref 47. These spectra show besides the IV-CT band at ~7000−8000 cm^{-1} a second band at ~11 000 cm^{-1} associated with the triarylamine to bridge hole transfer. In the much more polar MeCN, the IV-CT band of $\mathbf{1}^+$ and of $\mathbf{2}^+$ is shifted to much higher energies, as is expected for a localized MV system due to the increase of the solvent reorganization energy in MeCN versus CH_2Cl_2 (see Figure 5 for the spectra of $\mathbf{1}^+$). In MeCN, the bridge band is not visible due to severe band overlap which also precludes band deconvolution and proper analysis.[61] Thus, we only state here that the pronounced IV-CT solvatochromism proves the localized nature of $\mathbf{1}^+$ and $\mathbf{2}^+$.

The situation is much different for $\mathbf{3}^+$ and $\mathbf{4}^+$. Even if we take the AM1-CISD computed quantities as very approximate, we have strong experimental evidence that $\mathbf{3}^+$ is indeed a valence delocalized system: if the diagram in Figure 3 is valid for $\mathbf{3}^+$, destabilization of the triarylamine localized states should increase the transition energy $\tilde{\nu}_a$. Therefore, we synthesized the radical cation $\mathbf{4}^+$ which has Cl substituents instead of MeO attached to the triphenylamine moieties because the Cl acceptors should destabilize positive charge at the triarylamine units.[62,63] The spectra of the radical cations $\mathbf{3}^+$ and $\mathbf{4}^+$ are given in Figure 5. Deconvolution of the experimental spectra of $\mathbf{3}^+$ and $\mathbf{4}^+$ in CH_2Cl_2 was done in the following way: In total, four Gaussian curves were used for the spectra fitting. The first Gaussian was fitted to the band at the lowest energy (hereafter called the CT band) in a way that the Gaussian peak superimposes the experimental peak maximum. The next two Gaussians were used to fit the high-energy side of the CT band, and the fourth Gaussian was used to fit the first peak maximum at ~11 000 cm^{-1}. For determining the transition moment μ_{ga}, we only used the first Gaussian. In Figure 5, one can estimate for $\mathbf{3}^+$ but more

CHART 2: AM1-CISD Optimized Gas Phase Structures (Angstroms) of 1^+, 2^+, and 3^+ and Ground State Coulson Charge Differences in a Solvent with $\epsilon = 2.0$ ($\Delta\rho = \rho(M^+) - \rho(M)$) Given as Black Circles ($\Delta\rho > 0$) and Gray Circles ($\Delta\rho < 0$)[a]

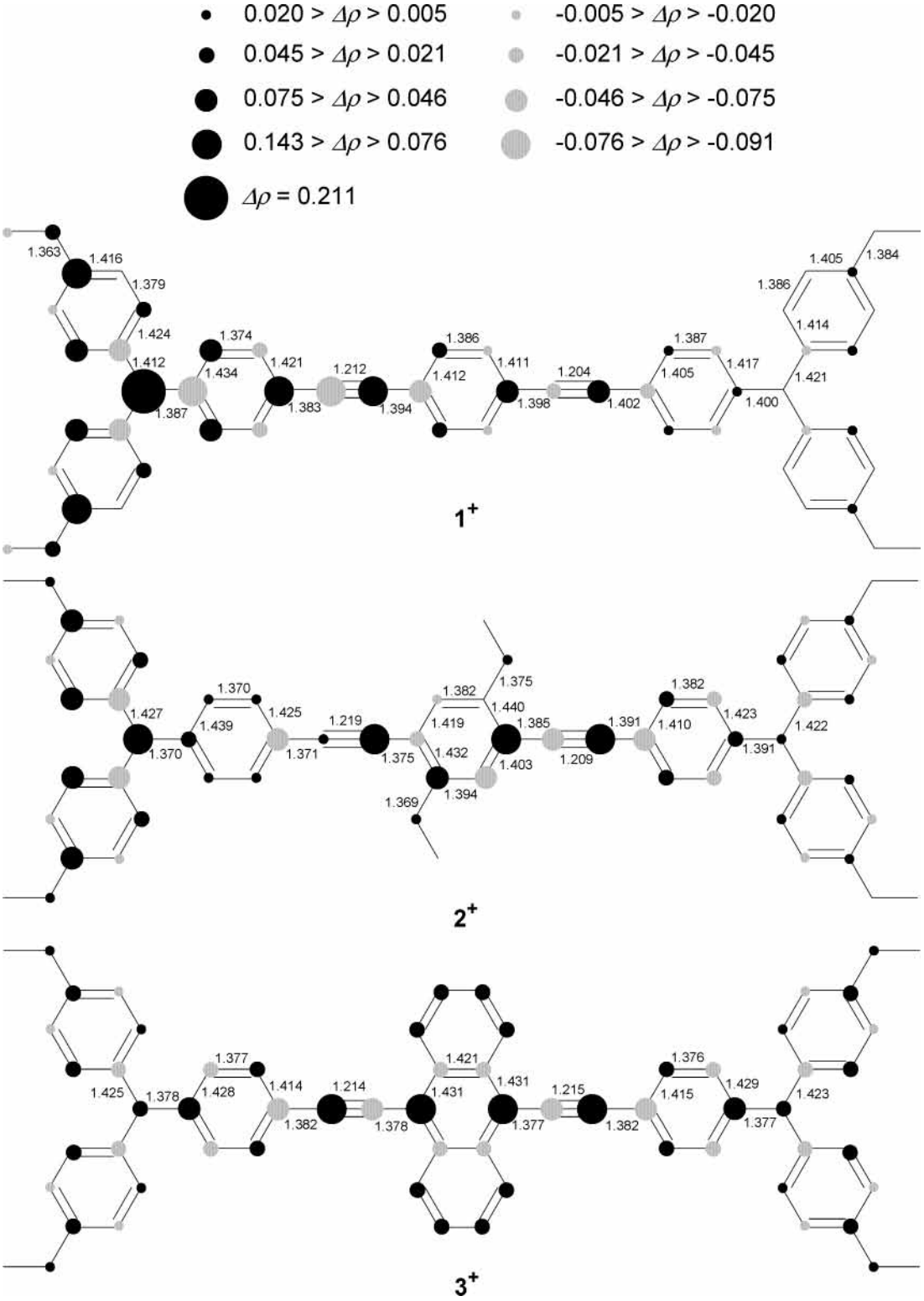

[a] The charge differences at the hydrogen atoms are quite small and are omitted.

clearly for $\mathbf{4}^+$ that there is a weak shoulder at the high-energy side of the CT band at ~6000−7000 cm^{-1}. This shoulder might actually be due to the forbidden transition $\tilde{\nu}_b$ (see section B) which might be weakly allowed by vibrational coupling. Therefore, the maximum of the second Gaussian was used to estimate the $\tilde{\nu}_b$ value (see Table 1) of $\mathbf{3}^+$. By this analysis, we found indeed that the CT transition energy is much higher in $\mathbf{4}^+$ (5500 cm^{-1}, $\mu_{ga} = 14.2$ D) than in $\mathbf{3}^+$ (4640 cm^{-1}). The contrary should be observed if $\mathbf{3}^+$ were valence localized and Figure 2 were the adequate description.

The second proof for the valence delocalized nature of $\mathbf{3}^+$ and $\mathbf{4}^+$ is the band shape of an excitation to a much higher lying state than $\tilde{\nu}_a$ or $\tilde{\nu}_b$ (Figure 5). This band at 11 300 cm^{-1} shows the same vibrational fine structure as 9,10-substituted

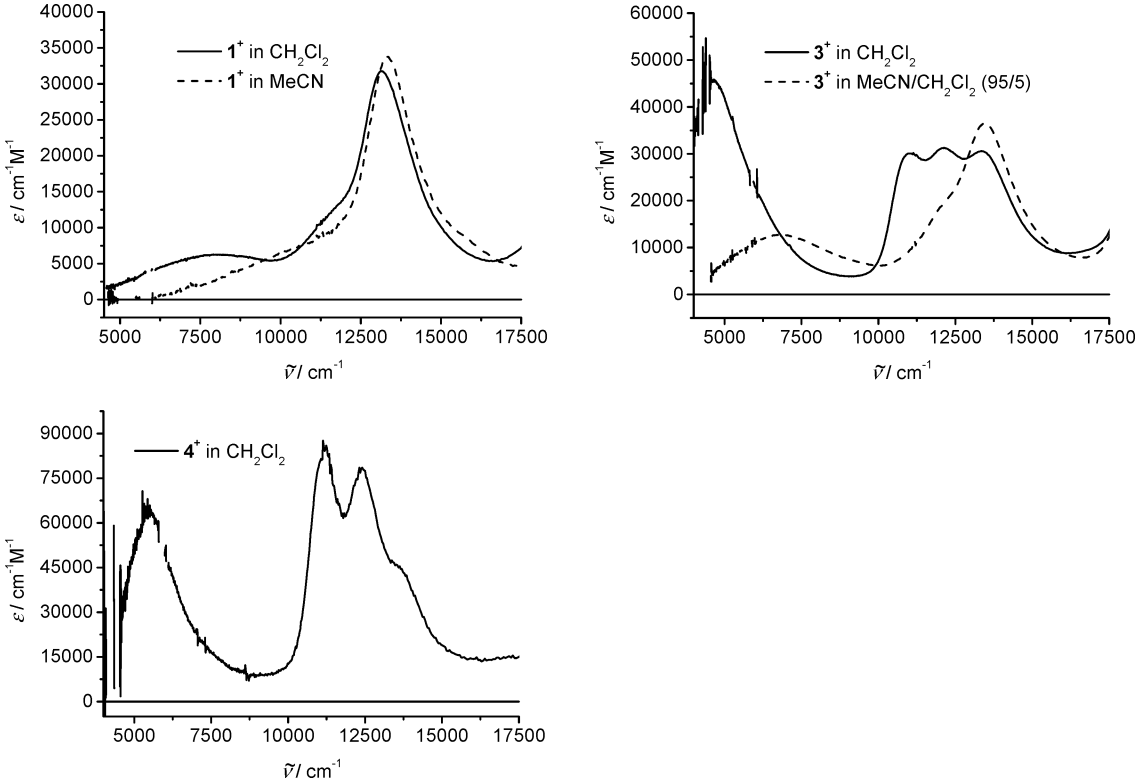

Figure 5. vis/NIR spectra of $\mathbf{1}^+$, $\mathbf{3}^+$, and $\mathbf{4}^+$.

anthracene radical cations[64] which also demonstrates that the charge is in part localized at the anthracene bridge in $\mathbf{3}^+$ and $\mathbf{4}^+$.

In contrast to $\mathbf{1}^+$, which shows a pronounced solvatochromism of the IV-CT band when measured in CH_2Cl_2 and MeCN, $\mathbf{3}^+$ shows a much different behavior. While its IV-CT band is narrow and at low energy in CH_2Cl_2, due to the symmetrical delocalized structure, the spectrum in MeCN shows a very broad IV-CT band at much higher energy (6770 cm^{-1}) as well as a bridge band as a shoulder at 12 300 cm^{-1} very similar to the ones observed for $\mathbf{1}^+$ and $\mathbf{2}^+$. In addition, the characteristic band of a localized triarylamine radical cation appears at 13 500 cm^{-1}. Obviously, $\mathbf{3}^+$ becomes asymmetrically localized in polar solvents. Spectrum deconvolution by four Gaussian curves yields $\mu_{ga} = 9.0$ D and $\mu_{gb} = 5.6$ D. Application of the three-level GMH analysis was impossible because we were unable to calculate the missing adiabatic transition moments.[65] However, if we estimate that the adiabatic dipole moment difference is $\mu_{aa} - \mu_{gg} = 60$ D, which is similar to the value for $\mathbf{1}^+$ in CH_2Cl_2, and apply the two-level approximation (eq 2), we obtain $V = 1020$ cm^{-1} for $\mathbf{3}^+$ in MeCN.

One could argue that using a bridge unit that is more easily oxidized than the terminal redox centers will lead to a symmetrical radical cation which hardly can be termed "valence delocalized" in the strict sense but might be named "bridge localized". However, in our case, the isolated bridge itself has a much higher oxidation potential (anthracene, $E_0 = 0.90$ V vs Fc/Fc^+ in MeCN)[66] than the triarylamines (trianisylamine, $E_0 = 0.16$ V vs Fc/Fc^+ in MeCN).[67] If only one donor is attached to anthracene, as in $\mathbf{5}^+$, it is the triarylamine center that is oxidized to yield the radical cation, as can be seen from the characteristic dianisylarylamine radical cation absorption at 13 550 cm^{-1} with a molar absorptivity of 37 900^{-1} M cm^{-1}.[47,68] The corresponding CT (triarylamine to anthracene) band in $\mathbf{5}^+$ is at a much higher energy (7740 cm^{-1}) but has approximately half the intensity ($\mu = 7.1$ D) of the absorption in $\mathbf{3}^+$. Therefore, the fact that the positive charge is delocalized in the anthracene unit and in the adjacent phenylethynyl substituents in $\mathbf{3}^+$ is a direct consequence of the donor substituents being attached to both the 9 and the 10 positions of anthracene. Thus, the symmetric ground state is a mixture of the anthracene centered state and the triarylamine centered states and, consequently, the term "valence delocalized" is appropriate. This means that valence delocalization can solely be induced by bridge modification without modification of the formal ET pathway or the distance of the redox centers.

D. Approximate GMH Theory for $\mathbf{3}^+$. The question remains of how to apply the GMH theory to valence delocalized systems such as $\mathbf{3}^+$ where important adiabatic transition moments such as μ_{ab} can be neither measured nor estimated accurately by computational methods. We do that by reducing the three-level model to two coupled two-level systems in the following way.

For symmetry reasons, the adiabatic and diabatic dipole moment matrices of valence delocalized $\mathbf{3}^+$ are the following:

$$\boldsymbol{\mu}_{\text{adiab}} = \begin{pmatrix} 0 & \mu_{ga} & 0 \\ \mu_{ga} & 0 & \mu_{ab} \\ 0 & \mu_{ab} & 0 \end{pmatrix}$$

and

$$\boldsymbol{\mu}_{\text{diab}} = \begin{pmatrix} 0 & 0 & 0 \\ 0 & \mu_{22} & 0 \\ 0 & 0 & \mu_{33} = -\mu_{22} \end{pmatrix}$$

$\boldsymbol{\mu}_{\text{adiab}}$ can be recast by a 45° rotation into the following similar matrix:

$$\boldsymbol{\mu}'_{\mathrm{adiab}} = \begin{pmatrix} 0 & \frac{\mu_{\mathrm{ga}}}{\sqrt{2}} & \frac{\mu_{\mathrm{ga}}}{\sqrt{2}} \\ \frac{\mu_{\mathrm{ga}}}{\sqrt{2}} & -\mu_{\mathrm{ab}} & 0 \\ \frac{\mu_{\mathrm{ga}}}{\sqrt{2}} & 0 & \mu_{\mathrm{ab}} \end{pmatrix}$$

which represents two coupled equivalent two-state models. We now assume that states a and b do not interact directly (tight binding approximation)[39] and therefore $\tilde{\nu}_a \approx \tilde{\nu}_b$. The adiabatic dipole moment $\mu_{ab} = \mu_{aa} - \mu_{gg} = -\mu_{bb} - \mu_{gg}$ now refers to the dipole moment difference between the ground state and either state a or state b. Applying the GMH unitary transformation with $\tilde{\nu}_a \approx \tilde{\nu}_b = 4640$ cm^{-1}, $\mu_{ga} = 14.1$ D, and $\mu_{ab} = 32$ D (estimated as one-half of the AM1-CI calculated $\mu_{aa} - \mu_{gg}$ value in CH_2Cl_2 for $\mathbf{1}^+$ (63.4 D) which also equals the $|\mu_{ab}|$ value for $\mathbf{3}^+$ in CH_2Cl_2 (33.1 D), see Table 1) yields $|V_{12}| = |V_{13}| = 1210$ cm^{-1} and $|V_{23}| = 380$ cm^{-1}. The matrix element for direct coupling (V_{12}) is similar to the averaged coupling (($|V_{13}| + |V_{23}|$)/2) of $\mathbf{1}^+$ (1070 cm^{-1}) and $\mathbf{2}^+$ (1270 cm^{-1}) but significantly lower than $|V_{12}| = |V_{23}| = 1660$ cm^{-1} of $\mathbf{3}^+$ if the GMH transformation without tight binding approximation and the matrix elements given in Table 1 are applied. Even in the tight binding approximation, there is a non-negligible coupling of $|V_{23}| = 380$ cm^{-1} between the triarylamine centered states which leads to a splitting of the excited state potentials a and b at $x = 0$. This coupling is similar in the tight binding approximation and the full three-level treatment (430 cm^{-1})

E. PES Parameter Fitting by Spectra Simulation. Using the electronic couplings evaluated by the GMH theory, we modeled the PESs for $\mathbf{1}^+$, $\mathbf{2}^+$, and $\mathbf{3}^+$ by diagonalizing the secular determinant 5.[47] This determinant is the three-level analogue to eq 1. In addition to the averaged asymmetric ET mode (x), a second averaged symmetric mode (y) is necessary to expand the PES in three dimensions. While the asymmetric mode localizes the charge on one of the two terminal redox centers (triarylamine units), the symmetric mode localizes the charge at the bridge. Similar two-level, two-mode models have been used quite successfully since 1980 by Hush,[69,70] Schatz,[71,72] Piepho,[73] Ondrechen,[40,41] and Zink.[74] For the construction of the PES, we place two diabatic potential functions for the triarylamine centered states augmented by quartic terms (weighted by the factor C)[27,75] at the corner of a triangle, while at the third corner the quadratic bridge state potential is placed. The latter potential is shifted in energy versus the minimum of the triarylamine centered states by $\Delta G°$. The quartic terms in the triarylamine centered potentials allow the potential curves to be more flexible. We chose different force constants (reorganization energies) (λ's) for the two different types of potentials (λ_1 for triarylamine centered states and λ_2 for the bridge state), but each type has the same force constant for the two different modes (symmetric and asymmetric). Of course, different reorganization energies[76] for the two coordinates would physically be more appropriate but would also lead to too many variables to be optimized. The coupling between the two triarylamine centered diabatic states was mediated by V_{IV} while the averaged coupling $V_{Br} = (|V_{13}| + |V_{23}|)/2$ was used for the coupling between the bridge state and both triarylamine centered states (see Table 2). When using an average coupling, one neglects the dependence of V on the ET coordinate (Condon approximation). Diagonalization of determinant 5 with an initially chosen set of parameters (λ_1, λ_2, C, and $\Delta G°$) gives the PES of the ground state, the excited bridge, and the IV-CT state. Assuming infinitely small spaced vibronic levels at the ground state PES and a Boltzmann distribution of states, we calculated the absorption spectrum to the bridge and IV-CT states in a classical manner.[71] Only three parameters, λ_1, λ_2, and $\Delta G°$ (and in the case of $\mathbf{1}^+$, C), were tuned in order to obtain a best fit to the Gaussian bands of the deconvoluted experimental absorption spectrum taken from ref 47. Because these parameters only weakly depend on each other, a reasonably good fit is readily achievable in this way.

The parameters used to fit the spectra (Figure 6) are collected in Table 2. The ground state PESs derived from these fits are depicted in Figure 7 as contour plots. Although the electronic couplings have changed significantly compared to our analysis in ref 47, the PES parameters for $\mathbf{1}^+$ did not and those for $\mathbf{2}^+$ did in the TS region only. While $\mathbf{1}^+$ shows a two minimum PES with the bridge state being a bay in the PES, $\mathbf{2}^+$ displays a distinct triple minimum PES with the bridge state as the third minimum on the ground state PES. This third minimum is the result of a low bridge state energy ($\Delta G° = 900$ cm^{-1}) combined with a relatively high reorganization energy of the 2,5-dimethoxyphenylene bridge which shows a quinoidal distortion upon oxidation.[46,77] As we have outlined in ref 47, this PES topology provides the possibility for a hopping ET mechanism between the triarylamine centered states via the bridge state as an alternative to the direct superexchange mechanism. Much in contrast, the negative diabatic $\Delta G°$ value in $\mathbf{3}^+$ makes the bridge state the only minimum on the ground state PES yielding a valence delocalized structure. As explained in section E, this negative $\Delta G°$ value is a consequence of the donor substitution of anthracene because anthracene itself has a much higher oxidation potential than triarylamines. An equally good fit to the experimental spectrum could also be obtained if two different reorganization energies of the triarylamine centered states were used for the asymmetric and symmetric coordinate, with $\lambda_{1x} = 6000$ cm^{-1} being much higher than $\lambda_{1y} = 3000$ cm^{-1}, while $\lambda_2 = 3000$ cm^{-1} has not been changed and $\Delta G° = -1400$ cm^{-1} has only slightly increased. This demonstrates that in the case of a valence delocalized bridge state minimum structure it is the symmetric coordinate that dominates the spectral features and not the asymmetric coordinate. In contrast to what one could expect from Figure 3, the excited state PES has no double minimum, owing to the rather strong coupling. If a much smaller coupling (e.g., $V_{Br} < 1000$ cm^{-1}) is used for the PES simulation, a double minimum, as indicated in Figure 3, appears.

Conclusions

In section A, we investigated the influence of different transition moments and transition energies on the electronic coupling in the context of a three-level model without tight

$$\begin{vmatrix} \lambda_1\left(\frac{x^2 + Cx^4 + y^2 + Cy^4}{1 + C}\right) - \epsilon & V_{Br} & V_{IV} \\ V_{Br} & \lambda_2\left[\left(\frac{1}{2} - x\right)^2 + \left(\frac{\sqrt{3}}{2} - y\right)^2\right] + \Delta G° - \epsilon & V_{Br} \\ V_{IV} & V_{Br} & \lambda_1\left[\frac{(1-x)^2 + C(1-x)^4 + y^2 + Cy^4}{1 + C}\right] - \epsilon \end{vmatrix} = 0 \quad (5)$$

TABLE 2: ET Parameters for 1^+, 2^+, and 3^+ in CH_2Cl_2 from the GMH Analysis and PES Fits

	V_{Br}[a]/cm^{-1}	V_{IV}[a]/cm^{-1}	λ_1[b]/cm^{-1}	C	λ_2[b]/cm^{-1}	$\Delta G°$ [b]/cm^{-1}	ΔG^* [c]/cm^{-1}
$\mathbf{1}^+$	$(\lvert V_{13}\rvert + \lvert V_{23}\rvert)/2 = 1070$	$V_{12} = 1000$	8500	0.2	3800	7600	1050
$\mathbf{2}^+$	$(\lvert V_{13}\rvert + \lvert V_{23}\rvert)/2 = 1270$	$V_{12} = 1910$	7400	0	9200	900	580 1780[d]
$\mathbf{3}^+$	$\lvert V_{12}\rvert = \lvert V_{13}\rvert = 1660$	$V_{23} = 430$	3000	0	3000	−1900	0

[a] ±20 cm^{-1}. [b] ±500 cm^{-1}. [c] ±100 cm^{-1}. [d] Minimum energy of the bridge state.

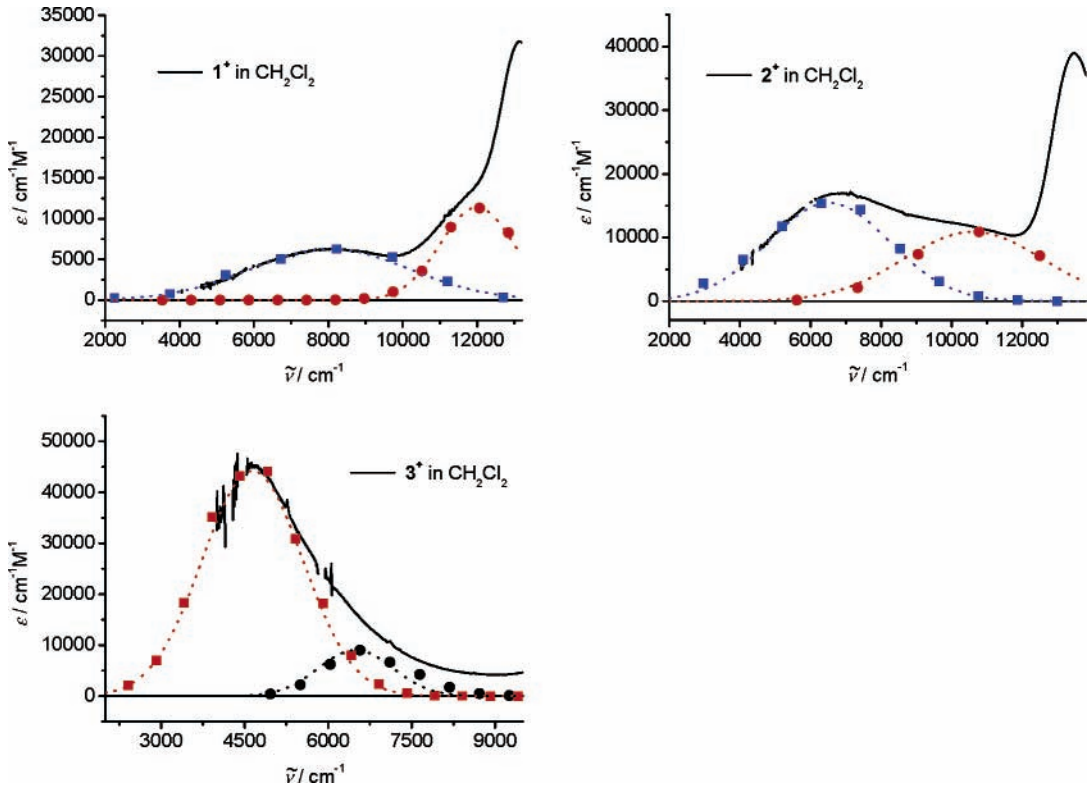

Figure 6. vis/NIR spectra of $\mathbf{1}^+$, $\mathbf{2}^+$, and $\mathbf{3}^+$ in CH_2Cl_2, deconvolution by Gaussian bands (dotted lines) and band fit (solid squares and solid circles) as described in text.

binding approximation. The most important outcome is that the much simpler two-level model is a good approximation only if the ratio of the adiabatic dipole moment difference between the terminal states and the sum of the two transition moments associated with the bridge state, $\Delta\mu_{ag}/(|\mu_{ab}| + |\mu_{gb}|)$, is larger than a threshold value depending on μ_{ga} and the transition energies. Because $\mu_{ga}/\Delta\mu_{ag}$ approximately screens the amount of charge localization,[78] this implies that the two-level model is only applicable to MV compounds in the Robin−Day class II with strongly localized redox states if qualitative correct values are desired. Even in the case of an energetically high-lying bridge excited state, the influence on the electronic coupling can be substantial if the transition moments associated with this bridge state are comparatively large (small $\Delta\mu_{ag}/(|\mu_{ab}| + |\mu_{gb}|)$ ratio). In most practical cases, the transition moments to bridge states are unknown because these bands strongly overlap with other bands or are completely hidden.

Using AM1-CI computations in section B, we studied three different bis(triarylamine) radical cations with varying bridge units. We found that the positive charge is more localized at the bridge the stronger the electron donating effect of the bridge is. For phenylene as the bridge ($\mathbf{1}^+$), the positive charge is mainly localized at one triarylamine unit, while, for 2,5-dimethoxyphenylene as the bridge ($\mathbf{2}^+$), the charge is delocalized between the bridge and one triarylamine moiety. Finally, for anthracene ($\mathbf{3}^+$), the charge is symmetrically delocalized over the anthracene bridge and both of the adjacent arylethynyl groups. Comparison of these three systems demonstrates that delocalization can be induced solely by bridge state modification, not by modifying the conjugation length or the conjugation type.

We used the three-level GMH theory to extract the electronic couplings from the above-mentioned AM1-CI calculations. We also performed the GMH transformation on the experimentally observed data complemented by the AM1 computed values where no experimental data are available. This analysis supports our above-made statement that the two-level model is a good approximation only if $\Delta\mu_{ag}$ is much larger than $|\mu_{ab}| + |\mu_{gb}|$. For the symmetrical anthracene bridged system $\mathbf{3}^+$, we also presented a coupled two-level model applying the tight binding approximation which is a reasonable approximation to the full three-level treatment.

In section C, the experimental vis/NIR spectra of the anthracene bridged system $\mathbf{3}^+$ in CH_2Cl_2 and in MeCN show a dramatic solvent influence. The analysis of the vis/NIR spectra revealed that the anthracene bridged system is symmetrically delocalized only in the weakly polar CH_2Cl_2 but asymmetrically localized in the polar MeCN. Solvent induced symmetry breaking has often been observed for neutral chromophores but is unprecedented to such an extent for MV compounds to our knowledge.

Using the electronic coupling evaluated by the GMH analysis, we constructed the adiabatic potential energy surfaces for the three bis(triarylamine) radical cations $\mathbf{1}^+$−$\mathbf{3}^+$ by using a semiclassical two-mode, three-level model. The potential energy surfaces show a double minimum potential for the strongly localized $\mathbf{1}^+$ (phenylene spacer) and a single minimum potential

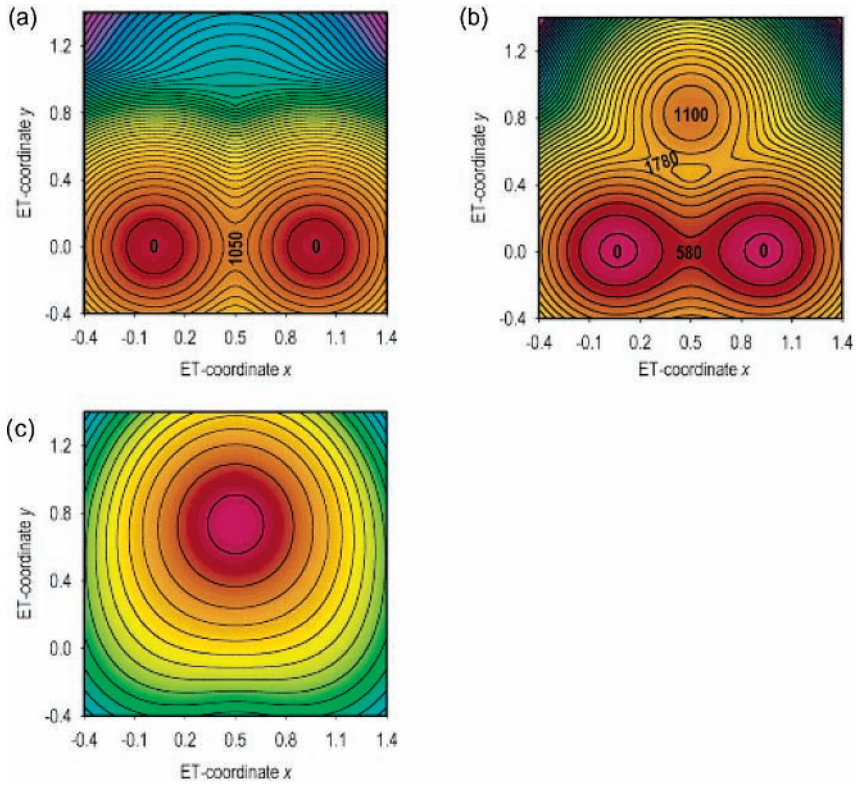

Figure 7. Ground state PES for (a) $\mathbf{1}^+$, (b) $\mathbf{2}^+$, and (c) $\mathbf{3}^+$ derived from eq 5. The contour lines have a separation of 250 cm^{-1}.

for the symmetrically delocalized $\mathbf{3}^+$ (anthracene spacer). This delocalization effect is due to the relatively low diabatic bridge state energy ($\Delta G°$) of donor substituted anthracene. The radical cation $\mathbf{2}^+$ with the 2,5-dimethoxyphenylene bridge displays a triple minimum potential where the bridge might serve as an intermediate state for a hopping mechanism as the alternative to a direct superexchange between the triarylamine centered states.

In conclusion, our study demonstrates that both the spectral features and the PES can solely be tuned by bridge state modification reaching from asymmetrically localized to symmetrically localized and from a single minimum potential to a triple minimum potential. For the particular case of the anthracene bridge, we showed that solvent induced symmetry breaking has a dramatic influence on the spectral characteristics. Unusual features of the anthracene bridge have been recognized earlier by several other authors.[43,79−83] Therefore, our study encourages us to reanalyze some older results in view of the outcome of the present work.

Methods

UV/vis/NIR Spectra. The vis/NIR spectra in CH_2Cl_2 were obtained by oxidizing an $\sim(1-5) \times 10^{-5}$ M solution of triarylamine compounds by dropwise addition of an $\sim 5 \times 10^{-3}$ M $SbCl_5/CH_2Cl_2$ solution. The spectra in MeCN were obtained by adding $NOBF_4$/MeCN solution in the same way. Because ET is rather slow using NO^+ in MeCN, one has to wait at least 1 h after the addition of a portion of the oxidizing agent before measuring the spectra. A spectrum with the IV-CT band at somewhat below maximal extinction (where practically no dication is present in equilibrium) was used, and its molar absorptivity was corrected by the comproportionation equilibrium as determined from cyclic voltammetry.

AM1 Calculations. All semiempirical calculations were done using the AM1 parametrization implemented in the MOPAC97 program.[84] The optimizations of all the structures were performed without symmetry restrictions in Cartesian coordinates by the eigenvector following (EF) method. Self-consistent field (SCF) convergence was achieved by Pulay's method. The configuration interaction included singles and doubles excitations (CISD) within an active orbital window comprising the four highest doubly occupied, one singly occupied, and three lowest unoccupied orbitals. The solvent influence on the optical properties was modeled by the COSMO method for a solvent with $\epsilon = 2.0$ and a solvent radius of 2.5 Å at the CISD optimized gas phase structures.

Acknowledgment. We are grateful to the Deutsche Forschungsgemeinschaft for financial support and to Prof. M. D. Newton (Brookhaven National Laboratory) for a thorough discussion on the three-level model.

References and Notes

(1) Newton, M. D. *Adv. Chem. Phys.* **1999**, *106*, 303−375.
(2) Cave, R. J.; Newton, M. D. *Chem. Phys. Lett.* **1996**, *249*, 15−19.
(3) Creutz, C.; Newton, M. D.; Sutin, N. *J. Photochem. Photobiol., A* **1994**, *82*, 47−59.
(4) Demadis, K. D.; Hartshorn, C. M.; Meyer, T. J. *Chem. Rev.* **2001**, *101*, 2655−2685.
(5) DeRosa, M. C.; White, C. A.; Evans, C. E. B.; Crutchley, R. J. *J. Am. Chem. Soc.* **2001**, *123*, 1396−1402.
(6) Lambert, C.; Nöll, G. *J. Am. Chem. Soc.* **1999**, *121*, 8434−8442.
(7) Brunschwig, B. S.; Creutz, C.; Sutin, N. *Chem. Soc. Rev.* **2002**, *31*, 168−184.
(8) Meacham, A. P.; Druce, K. L.; Bell, Z. R.; Ward, M. D.; Keister, J. B.; Lever, A. B. P. *Inorg. Chem.* **2003**, *42*, 7887−7896.
(9) Londergan, C. H.; Kubiak, C. P. *Chem.—Eur. J.* **2003**, *9*, 5962−5969.
(10) Neyhart, G. A.; Timpson, C. J.; Bates, W. D.; Meyer, T. J. *J. Am. Chem. Soc.* **1996**, *118*, 3730−3737.
(11) Nelsen, S. F. *Chem.—Eur. J.* **2000**, *6*, 581−588.
(12) Ito, T.; Hamaguchi, T.; Nagino, H.; Yamaguchi, T.; Washington, J.; Kubiak, C. *Science* **1997**, *277*, 660−663.
(13) Nelsen, S. F.; Ismagilov, R. F.; Trieber, D. A. *Science* **1997**, *278*, 846−849.

(14) Brunschwig, B. S.; Sutin, N. In *Electron Transfer in Chemistry*; Balzani, V., Ed.; Wiley-VCH: Weinheim, Germany, 2001; Vol. 2, pp 583−617.
(15) Hush, N. S. *Coord. Chem. Rev.* **1985**, *64*, 135−157.
(16) Crutchley, R. J. *Adv. Inorg. Chem.* **1994**, *33*, 273−325.
(17) Creutz, C. *Prog. Inorg. Chem.* **1983**, *30*, 1−73.
(18) Launay, J.-P. *Chem. Soc. Rev.* **2001**, *30*, 386-397.
(19) Brunschwig, B. S.; Creutz, C.; Sutin, N. *Coord. Chem. Rev.* **1998**, *177*, 61−79.
(20) Vance, F. W.; Slone, R. V.; Stern, C. L.; Hupp, J. T. *Chem. Phys.* **2000**, *253*, 313−322.
(21) Bublitz, G. U.; Laidlaw, W. M.; Denning, R. G.; Boxer, S. G. *J. Am. Chem. Soc.* **1998**, *120*, 6068−6075.
(22) Nelsen, S. F.; Newton, M. D. *J. Phys. Chem. A* **2000**, *104*, 10023−10031.
(23) Nelsen, S. F.; Konradsson, A. E.; Weaver, M. N.; Telo, J. P. *J. Am. Chem. Soc.* **2003**, *125*, 12493−12501.
(24) Coropceanu, V.; Malagoli, M.; André, J. M.; Brédas, J. L. *J. Am. Chem. Soc.* **2002**, *124*, 10519−10530.
(25) Coropceanu, V.; Lambert, C.; Nöll, G.; Brédas, J.-L. *Chem. Phys. Lett.* **2003**, *373*, 153−160.
(26) Low, P. J.; Paterson, M. A. J.; Puschmann, H.; Goeta, A. E.; Howard, J. A. K.; Lambert, C.; Cherryman, J. C.; Tackley, D. R.; Leeming, S.; Brown, B. *Chem.−Eur. J.* **2004**, *10*, 83−91.
(27) Nelsen, S. F.; Ismagilov, R. F.; Gentile, K. E.; Powell, D. R. *J. Am. Chem. Soc.* **1999**, *121*, 7108−7114.
(28) Chen, P.; Meyer, T. J. *Chem. Rev.* **1998**, *98*, 1439−1478.
(29) Nelsen, S. F.; Trieber, D. A.; Ismagilov, R. F.; Teki, Y. *J. Am. Chem. Soc.* **2001**, *123*, 5684−5694.
(30) Nelsen, S. F.; Tran, H. Q. *J. Phys. Chem. A* **1999**, *103*, 8139−8144.
(31) Hupp, J. T.; Dong, Y.; Blackbourn, R. L.; Lu, H. *J. Phys. Chem.* **1993**, *97*, 3278−3282.
(32) Nelsen, S. F.; Ismagilov, R. F. *J. Phys. Chem. A* **1999**, *103*, 5373−5378.
(33) Blackbourn, R. L.; Hupp, J. T. *J. Phys. Chem.* **1990**, *94*, 1788−93.
(34) Rust, M.; Lappe, J.; Cave, R. J. *J. Phys. Chem. A* **2002**, *106*, 3930−3940.
(35) Reimers, J. R.; Hush, N. S. *J. Phys. Chem. A* **1999**, *103*, 3066−3072.
(36) Reimers, J. R.; Hush, N. S. *Chem. Phys.* **1989**, *134*, 323−354.
(37) Petrov, E. G.; Shevchenko, Y. V.; May, V. *Chem. Phys.* **2003**, *288*, 269−279.
(38) Davis, W. B.; Wasielewski, M. R.; Ratner, M. A.; Mujica, V.; Nitzan, A. *J. Phys. Chem. A* **1997**, *101*, 6158−6164.
(39) Newton, M. D. *Chem. Rev.* **1991**, *91*, 767−792.
(40) Ko, J.; Ondrechen, M. J. *J. Am. Chem. Soc.* **1985**, *107*, 6161−6167.
(41) Root, L. J.; Ondrechen, M. J. *Chem. Phys. Lett.* **1982**, *93*, 421−424.
(42) Londergan, C. H.; Kubiak, C. P. *J. Phys. Chem. A* **2003**, *107*, 9301−9311.
(43) Nelsen, S. F.; Ismagilov, R. F.; Powell, D. R. *J. Am. Chem. Soc.* **1998**, *120*, 1924−1925.
(44) Milischuk, A.; Matyushov, D. V. *J. Chem. Phys.* **2003**, *118*, 5596−5606.
(45) Le Stang, S.; Paul, F.; Lapinte, C. *Organometallics* **2000**, *19*, 1035−1043.
(46) Lindeman, S. V.; Rosokha, S. V.; Sun, D.; Kochi, J. K. *J. Am. Chem. Soc.* **2002**, *124*, 843−855.
(47) Lambert, C.; Nöll, G.; Schelter, J. *Nat. Mater.* **2002**, *1*, 69−73.
(48) Cave, R. J.; Newton, M. D.; Kumar, K.; Zimmt, M. B. *J. Phys. Chem.* **1995**, *99*, 17501−17504.
(49) Cave, R. J.; Newton, M. D. *J. Chem. Phys.* **1997**, *106*, 9213−9226.
(50) Shin, Y.-G. K.; Newton, M. D.; Isied, S. S. *J. Am. Chem. Soc.* **2003**, *125*, 3722−3732.
(51) Jones, G. A.; Carpenter, B. K.; Paddon-Row, M. N. *J. Am. Chem. Soc.* **1999**, *121*, 11171−11178.
(52) Nelsen, S. F.; Blomgren, F. *J. Org. Chem.* **2001**, *66*, 6551−6559.
(53) Dewar, M. J. S.; Hashmall, J. A.; Venier, C. G. *J. Am. Chem. Soc.* **1968**, *90*, 1953−1957.
(54) Although methylene chloride which was used in the experiments has $\epsilon = 8.9$, we empirically chose a much lower permittivity because the COSMO method tends to overestimate strongly the solvent influence on the CT energies in polar solvents; e.g., AM1-CISD/COSMO calculations on $\mathbf{1}^+$ with $\epsilon = 8.9$ and a solvent radius of 2.9 Å yield the following excitation energies and transition moments: $\tilde{\nu}_a = 12\,680$ cm^{-1} and $\tilde{\nu}_b = 16\,580$ cm^{-1} as well as $\mu_{gg} = -42.6$ D, $\mu_{aa} = 7.3$ D, $\mu_{bb} = 6.7$ D, $\mu_{ga} = -12.4$ D, $\mu_{gb} = 4.9$ D, and $\mu_{ab} = -8.6$ D. For more details about the application of the COSMO method to excited states, see: Klamt, A. *J. Phys. Chem.* **1996**, *100*, 3349−3353.
(55) The dipole moment of ions is not uniquely defined. We chose the center of gravity as the origin of the dipole moment vector which is equivalent to the center of the bridge.
(56) At the UHF level, all radical cations show strong charge localization at one triarylamine center and an asymmetrical structure. This broken symmetry effect is an inherent artifact of the UHF method.
(57) The experimental ionization potential (IP) of triphenylamine (6.80 eV)[85] is distinctly smaller than that of anthracene (7.45 eV),[85] while this difference is much smaller if AM1 values are used (7.97 eV for triphenylamine and 8.12 eV for anthracene according to Koopman's theorem). This fact also prohibits the optimization of $\mathbf{3}^+$ in MeCN which should lead to a triarylamine localized asymmetric structure according to our experimental observations but remains in fact symmetrically delocalized.
(58) Matyushov, D. V.; Voth, G. A. *J. Phys. Chem. A* **2000**, *104*, 6470−6484.
(59) We were unable to calculate the corresponding transition moments at the symmetrical neutral structure instead of the true symmetrical transition structure because the wave function showed a broken symmetry effect. Neutral structures were used by Coropceanu et al.[24] previously in order to estimate $\mu_{22} - \mu_{11}$.
(60) Although the coupling quantities evaluated in this paper are significantly different from those given in ref 47, the PES parameters of all compounds with the exception of $\mathbf{3}^+$ and the conclusions concerning the bridge mediated hopping remain valid because the electronic coupling has only a minor influence on the topology of the PES in these cases.
(61) Compound $\mathbf{1}^+$ decomposes in MeCN within hours, which precludes the accurate determination of the molar absorptivity by our titration experiments with $NOBF_4$. However, the band assigned to the localized dianisylarylamine radical cation excitation at ~13 330 cm^{-1} has a molar absorptivity of ~33 800 M^{-1} cm^{-1}, which compares very well with those of other triarylamine radical cations such as the trianisylamine radical cation (13 710 cm^{-1}, $\epsilon = 33\,800$ M^{-1} cm^{-1} in CH_2Cl_2). We therefore conclude that the molar absorptivity of $\mathbf{1}^+$ in Figure 5 is accurate to ~ ±10%.
(62) Lambert, C.; Nöll, G. *J. Chem. Soc., Perkin Trans. 2* **2002**, 2039−2043.
(63) Schelter, J. Ph.D. Thesis, Universität Würzburg, 2003.
(64) Shida, T. *Electronic Absorption Spectra of Radical Ions*; Elsevier: Amsterdam, The Netherlands, 1988.
(65) Optimization of $\mathbf{3}^+$ in MeCN solvent by the COSMO method gave a symmetrical structure similar to the one in the gas phase. We assume this to be an artifact of the AM1 parametrization, as explained in footnote 57.
(66) Knorr, A. Ph.D. Thesis, University of Regensburg, 1995.
(67) Dapperheld, S.; Steckhan, E.; Brinkhaus, K.-H. G.; Esch, T. *Chem. Ber.* **1991**, *124*, 2557−2567.
(68) In our older publications, we assigned this transition to a $\pi-\pi$ excitation of triarylamine radical cations in general. We now observed that this excitation is only observed for trianisylamine and dianisylarylamine radical cations at that particular position and intensity.
(69) Hush, N. S. In *Mixed-Valence Compounds*; Brown, D. B., Ed.; D. Reidel Publishing Company: Dordrecht, The Netherlands, 1980; pp 151−188.
(70) Reimers, J. R.; Hush, N. S. *Chem. Phys.* **1996**, *208*, 177−193.
(71) Wong, K. Y.; Schatz, P. N. *Prog. Inorg. Chem.* **1981**, *28*, 369−449.
(72) Schatz, P. N. In *Mixed Valency Systems: Applications in Chemistry, Physics and Biology*; Prassides, K., Ed.; Kluwer Academic Publishers: Dordrecht: The Netherlands, 1991; pp 7−28.
(73) Piepho, S. B. *J. Am. Chem. Soc.* **1988**, *110*, 6319−6326.
(74) Talaga, D. S.; Zink, J. I. *J. Phys. Chem. A* **2001**, *105*, 10511−10519.
(75) Nelsen, S. F.; Ismagilov, R. F.; Powell, D. R. *J. Am. Chem. Soc.* **1997**, *119*, 10213−10222.
(76) Small, D. W.; Matyushov, D. V.; Voth, G. A. *J. Am. Chem. Soc.* **2003**, *125*, 7470−7478.
(77) Rathore, R.; Lindeman, S. V.; Kumar, A. S.; Kochi, J. K. *J. Am. Chem. Soc.* **1998**, *120*, 6931−6939.
(78) Within the two-level model, the delocalization parameter $\Delta z = [1 + 4\mu_{ga}^2/\Delta\mu_{ag}^2]^{-1/2}$; see ref 58.
(79) Karafiloglou, P.; Launay, J.-P. *Chem. Phys.* **2003**, *289*, 231−242.
(80) El-ghayoury, A.; Harriman, A.; Khatyr, A.; Ziessel, R. *J. Phys. Chem. A* **2000**, *104*, 1512−1523.
(81) Kilså, K.; Kajanus, J.; Macpherson, A. N.; Mårtensson, J.; Albinsson, B. *J. Am. Chem. Soc.* **2001**, *123*, 3069−3080.
(82) Holzapfel, M.; Lambert, C.; Selinka, C.; Stalke, D. *J. Chem. Soc., Perkin Trans. 2* **2002**, 1553−1561.
(83) Fraysse, S.; Coudret, C.; Launay, J.-P. *J. Am. Chem. Soc.* **2003**, *125*, 5880−5888.
(84) Stewart, J. J. P. *MOPAC97*; Fujitsu Limited: 1997.
(85) NIST Chemistry WebBook, NIST Standard Reference Database Number 69; Linstrom, P. J., Mallard, W. G., Eds.; National Institute of Standards and Technology: Gaithersburg, MD, March 2003 (http://webbook.nist.gov).